Left Ventricle Tracking in CMR Images for Measuring Myocardial Extracellular Volume Fraction

Hua Zhong, PhD* Tim Wong, MD† Christopher G Meier† Stephen M Testa†
Willima Ceyrolles, MD† Joshua Levenson† Erik Schelbert, MS,MD†

*Spotlight Medical Inc.
† University of Pittsburgh Medical Center

ABSTRACT

A computer-assisted tool to efficiently locate left ventricle myocardium centerline contour from short-axis MOLLI sequence of CMR images using a global and local shape tracking algorithm is presented in this paper. The algorithm can track both the changing of ventricle shape due to respiratory motion and the changing of pixel values due to different TI time when an image is scanned through the MOLLI sequence. It increases the measurement efficiency by automating the myocardial extracellular volume fraction V_e calculation for left ventricle, which is important to characterize adverse myocardial remodeling.

Index Terms: I.2.10 [Vision and Scene Understanding]: Motion—Tracking; I.4.8 [Scene Analysis]: Shape—Detection;

1 INTRODUCTION

Expansion of the myocardial interstitium characterizes adverse myocardial remodeling, and represents a final common pathway of myocardial injury [10]. Underscoring myocardial remodeling as a therapeutic target, pharmacologic interventions to reverse myocardial remodeling also reverse the risks of adverse cardiovascular outcomes [3]. Cardiovascular magnetic resonance (CMR) can quantify the myocardial interstitium accurately, providing novel structural parameters to monitor myocardial interstitial expansion directly [4] [6]. CMR quantifies myocardial interstitial expansion by measuring the extracellular volume fraction (V_e) and the partition coefficient (λ_{Gd}) of (extracellular) gadolinium contrast agent [6] [8]: After intravenous bolus or infusion, Gd contrast accumulates in areas of extracellular matrix expansion, proportionally shortening myocardial $T1$ relaxation [9]. By measuring the T_1 value for both blood and myocardium before and after the injection of Gd contrast, we can calculate the λ_{Gd} by:

$$\lambda_{Gd} = (\frac{1}{T_{1_{preblood}}} - \frac{1}{T_{1_{postblood}}})/(\frac{1}{T_{1_{premyo}}} - \frac{1}{T_{1_{postmyo}}}) \quad (1)$$

where $T_{1_{preblood}}$ and $T_{1_{postblood}}$ are the T_1 relaxation time for blood before and after the injection of contrast. While $T_{1_{premyo}}$ and $T_{1_{postmyo}}$ are the T_1 for myocardium before and after the injection. Then the myocardial extracellular volume fraction V_e can be calculated by:

$$V_e = \lambda_{Gd} * \rho * (1 - Hct) - V_p \quad (2)$$

where V_p is the myocardial plasma volume fraction (typically assumed to be 0.045), ρ is the specific density of myocardial tissue (1.05 ml/g), and Hct is the hematocrit measured during blood test for the patient.

*e-mail: hua.zhong@gmail.com

T_1 measurement, the basis for V_e measures, is most efficiently performed with a modified Look-Locker inversion recovery (MOLLI) pulse sequence. Yet the post processing time for these measurements of myocardial remodeling is a significant barrier that prevents their widespread application. The majority of the time is spent on manually identify myocardium contours in MOLLI sequence and hand pick sample pixels for T_1 calculation. Therefore, there is a great need to create tools to expedite the process.

We present a computer-assisted tool to efficiently locate left ventricle myocardium from a short-axis MOLLI sequence using a global and local shape tracking algorithm. The algorithm can track the changing of ventricle shape due to small respiratory motion and automates V_e value calculation. It can calculate V_e for both the whole myocardium and for different sections of the left ventricle which gives not only the general global healthy index but also local health measurements of the left ventricle , which will be very helpful for future procedures to prevent and reverse myocardial remodeling.

2 TRACKING LEFT VENTRICLE IN SHORT-AXIS MOLLI SEQUENCE

With most CMR images, MOLLI sequence is captured while the person being scanned is holding his/her breath. In this way, usually there is no significant respiratory motion. However small motions still exist due to differences among multiple breath-holdings and failing to hold the breath steady. With respiratory motions, a left ventricle moves both rigidly and changes shape non-rigidly through the MOLLI sequence. In order to correctly calculate the T_1 value, we need exact correspondences of sample pixels across all images in a MOLLI sequence, so we need to track the shape and location of left ventricle.

In MOLLI sequences, each image is captured at different cardiac cycles and with different TI (inversion time) times. Thus the same tissue shows different pixel values across the sequence, as shown in Figure 1. The assumption of frame-to-frame coherence for most tracking algorithms is not entirely true in this case then. However the tracking by detecting paradigm works well here: we detect left ventricle independently in each frame of a MOLLI sequence given a universal initialization. With local features designed to track changing tissue colors and a global+local tracking algorithm, we are able to handle the special challenge of MOLLI sequences.

2.1 Local+Global Tracking Model

Our detection algorithm follows the local feature tracking plus global shape constraint model. Suppose we have a set of local feature models which each tracks certain part of the interested object:

$$L = \{L_1, L_2, ..., L_n\}$$

where each local feature L_i represents what the interested object looks like at a particular location of the global shape,

And a global shape model of the interested object is:

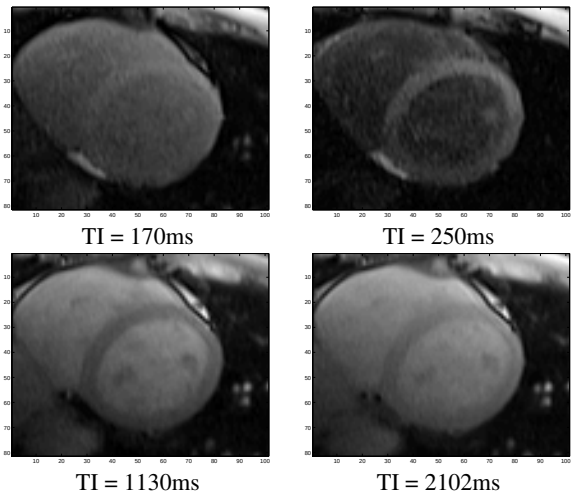

Figure 1: Some examples of short-axis CMR images from a MOLLI sequence. Note that images captured at different TI time have different pixel values for the same tissues. Near the end of the sequence (largest TI), all tissues tend to fade into a same color.

$$GlobalModel = G(a)$$

a is the parameter for this global shape model.

For an image I, the tracking (detecting) algorithm consists of two steps:

---

1. Find the (x_i, y_i) for each local feature L_i that maximizes the probability of $P((x_i, y_i)|I)$. Usually the likelihood instead is used for maximization using the Bayes' theorem:

$$\max_{(x_i,y_i)} P((x_i,y_i)|I) = \max_{(x_i,y_i)} \frac{P(I|(x_i,y_i))P(x_i,y_i)}{P(I)}$$

$$= \max_{(x_i,y_i)} P(I|(x_i,y_i))P(x_i,y_i) \quad (3)$$

   where $P(I|(x_i,y_i))$ is the likelihood of the image given feature L_i at location (x_i,y_i) and $P(x_i,y_i)$ is a prior for feature L_i to be located at (x_i,y_i).

2. After we have a set of optimal local feature locations $\{(x_i,y_i)\}, i = 1..n$, find a parameter set a_{opt} that maximizes

$$P(a|G,L,\{(x_1,y_1),(x_2,y_2),...,(x_n,y_n)\})$$

   which is the probability of global model parameter a given current local and global model and the best local feature locations. Similar to local features, it is usually done by maximizing the likelihood:

$$\max_a P((x_1,y_1),(x_2,y_2),...,(x_n,y_n)|a,G,L)P(a) \quad (4)$$

   And the shape generated by the optimal parameter a_{opt} $G(a_{opt})$ is our final result shape.

Many shape detecting or segmenting algorithms [1] [2] [7] can be considered implementing this two step model with different L, $G(a)$ and probabilities definitions. In the following sections we will detail these definitions used in our algorithm.

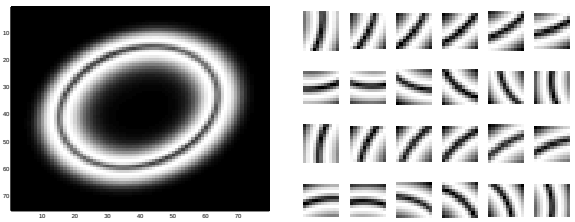

Figure 2: LV Template and local feature.

2.2 Local Feature Tracking

2.2.1 Definition of Local Feature L

Because the absolute pixel values for myocardium in MOLLI images change with TI time(as shown in Figure 1), we focus on the gradient image rather than the original gray scale image. In gradient image, as long as the pixel value of myocardium is different than the value of blood, we can observe high gradient values along the myocardium-blood border. Our local features are designed to capture the bright gradient values on both the endocardial and epicardial border. In short-axis MOLLI sequence, left ventricle's shape can be approximated by an ellipse. We derive our local features from an ellipse template created based on an initial global shape as shown in Figure 2(a). The initial shape is usually defined by user at the beginning of a tracking session. Along the ellipse shape, we sample n locations. The local features L are small sub-images cut from the ellipse-shaped template at the sample locations, as shown in Figure 2(b).

2.2.2 Definition of Local Feature Likelihood $P(I|(x_i,y_i))$

Given an image I, we first compute the gradient image I_g. For a local feature L_i, which is a small image patch as shown in Figure 2 (b), the likelihood of $P(I|(x_i,y_i))$ is defined as proportional to:

$$NorCorr(SubImg(I_g,x_i,y_i),L_i) \quad (5)$$

where $NorCorr(I_1,I_2)$ is the normalized cross-correlation of image I_1 and I_2 [5]. $SubImg(I,x_i,y_i)$ is the sub-image of I_g centered at location (x_i,y_i). It has the same size as the local feature L_i.

2.2.3 Definition of Prior $P(x_i,y_i)$

Given an initial feature location (x_{i0},y_{i0}), we define the prior probability of feature location (x_i,y_i) for feature L_i is proportional to:

$$e^{-d/a} \cdot S(d)Q(I(x_i,y_i)) \quad (6)$$

where $d = ||(x_{i0},y_{i0}),(x_i,y_i)||$ is the distance of (x_i,y_i) to the initial feature location. It means further the (x_i,y_i) is from initial location, lower the probability is. $S(d)$ is a function which returns 1 if d is lower than a certain threshold and 0 otherwise. It actually gives any locations that are farther than a certain threshold to the initial location zero probability. This helps us to focus the search of best feature location within a local neighborhood (determined by the threshold) of the initial feature location. a is a constant controlling how fast the probability drops with d increases. We also have knowledge of all possible myocardium pixel values in a MOLLI sequence. That information is encoded in function $Q(I(x_i,y_i))$. $I(x_i,y_i)$ is the pixel value at location (x_i,y_i). All impossible pixel values for myocardium will result a zero for $Q()$. $Q()$ will return 1 for all possible values.

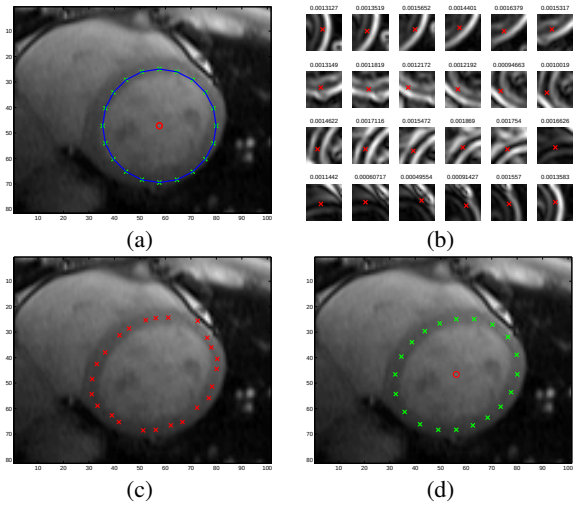

Figure 3: LV Detection (a) Initial shape usually is a circle defined by users. (b) Then the best location of each local feature is detected in the gradient image. (c) Result of local feature detection. Not all features are detected reliable due to local image ambiguities. (d) Final detection result by applying global shape constraint.

2.2.4 Maximize the $P(I|(x_i,y_i))P(x_i,y_i)$

With the definition given above, we can maximize the product of likelihood and prior by the following steps:

For a local feature L_i, its initial location (x_{i0},y_{i0}), and image I

1 At any location (x_i,y_i) within a certain threshold to (x_{i0},y_{i0}), cut a sub-image from gradient image Ig with the same size as L_i;

2 Calculate the normalized correlation of the sub-image and L_i, and multiply it with $P(x_i,y_i)$ as defined in Equation 6, and save the result as the "matching score" for the location;

3 For all the locations calculated, pick the one with best "matching score" as the final optimal feature location.

2.2.5 Scale of Local Features

To deal with the scale changes of local features due to various myocardium thickness, each local feature will be represented as a pyramid of the same feature with different scales. For example, we create a local feature and scaled it into 50%, 75%, 100%, 125%, and 150% images. During the tracking, each scaled feature will return a normalized best score. We pick the best one from all scales as the final score of the feature and the corresponding location as the new feature location.

At the beginning, a template is created based on either a user-defined initial shape, or a result of a previous image. Then multiple local features are cut from the template. The initial feature locations are also defined by the initial shape. For each feature, we find the new feature location by maximizing the likelihood as described above. The final result is a set of new best local feature locations $\{(x_1,y_1),(x_2,y_2),...,(x_n,y_n)\}$ for the next global constraint step, as shown in Figure 3(c).

2.3 Global Shape Constraint

2.3.1 Definition of Global Shape

We can reliably define the global shape model of LV in short-axis images G as an ellipse. A general form of ellipse equation can be written as:

$$G(a,x,y) = a_0x^2 + a_1y^2 + a_2x + a_3y + a_4xy - 1 = 0$$

and $a = \{a_0,a_1,a_2,a_3,a_4\}$ is the parameter set for the global shape G.

2.3.2 Maximize the Likelihood $P((x_i,y_i)|a,G,L)$

In our case, we define the prior of a $P(a)$ as constant. Then it can be ignored during the maximization. The likelihood of $P((x_i,y_i)|a,G,L)$ is defined as proportional to an exponential function of:

$$e^{-G(a,x_i,y_i)^2} \tag{7}$$

which means farther the point (x_i,y_i) is from the global model $G(a,x,y) = 0$, lower the likelihood is. Then the maximization of the joint likelihood of all (x_i,y_i) can be written as:

$$\max_a \Pi_i P((x_i,y_i)|a,G,L)$$

Replacing likelihood by Equation 7 and using the log likelihood, the above maximization equals to:

$$\min_a \sum_i G(a,x_i,y_i)^2$$

which can be solved by standard least square estimation. The optimal parameter set a_{opt} that maximizes the likelihood will be the result LV shape: $G(a_{opt},x,y) = 0$. It is possible that some local features are badly detected and the erroneous (x_i,y_i)'s corrupt the final global shape. To reduce this negative effect, we introduce weights $w = \{w_1,w_2,...,w_i\}$ based on each local feature's final matching score into the maximization of global shape likelihood:

$$\min_a \sum_i w_iG(a,x_i,y_i)^2$$

In this way, the badly detected local features, which usually have low matching scores, will not influence the final result as much as the reliably detected local features. As shown in Figure 3(d), an example of LV tracking result after global shape constraint, the noise of local feature detection results has been successfully smoothed out with global constraint.

2.4 Collaborative Detection

Sometimes, the fat around the epicardial border will attract gradient feature we used to wrong locations, especially for images captured with large TI value when edge between blood and myocardium is blurred. However, we found another set of features based on image pixel intensity works better for these cases.

2.4.1 Intensity-based Local Feature

Similar to the feature we defined in section 2.2.1, we create two sets of local features based on the template shown in Figure 4. Template (a) is designed to detect myocardium with blood on one side and air on the other side. While template (b) is to detect myocardium with blood on both sides. Each local feature L_i will contain multiple scaled sub-images cut from both templates. During local feature detection, features from both templates will be compared to the original intensity image I to compute the normalized correlation. Normalized correlation is insensitive to absolute pixel values, which is desired for images in MOLLI sequence. Instead of using the normalized correlation result directly, we use the absolute value to make the template can also detect the intensity-inverted features. This is important because, as we mentioned above, pixel values of MOLLI sequence constantly change with TI. Finally the one with highest "matching score" will be chosen as the final feature location.

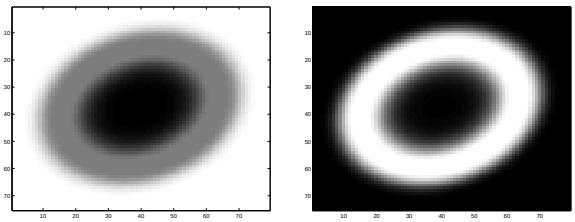

(a) (b)

Figure 4: Intensity based local feature templates. (a) to track myocardium with different materials on both sides. (b) to track myocardium with similar materials on both sides. We also use the absolute value of normalized correlation when comparing to image to track the feature that is inverted to the template.

2.4.2 Collaborative Detection

With m kinds of local features ($m = 3$ in our case since we have 2 intensity-based features and 1 gradient-based feature), each image I will have multiple detection results $G(a_k)$ for $k = 1,...,m$. We linearly combine these detection results to generate the final shape:

$$a_{final} = \frac{1}{R}\sum_{k=1}^{m} r_k a_k$$

where r_k is the mixing co-efficient for feature k and R is a normalization constant. For our case, equally mixing the gradient feature and pixel intensity feature gives us robust detection result. By collaborating, one feature can "correct" the wrongs of other features.

Figure 5 illustrates one example that collaborative detection improves both gradient and intensity feature results. Figure 5 (a) is the result based on gradient feature only. The upper right part of the contour is attracted by the fat in the epicardial border. (b) is the result from intensity feature, which is robust in the upper right part. However in the lower right part, the contour is quite close to the lung. (c) is the collaborative result which is more robust on both regions. (d) shows all 3 contours together.

2.5 Interactive Correction

An accurate initial contour benefits the subsequent tracking results. Also, some low quality images may cause sub-optimal tracking results. Images with little pixel value difference between blood and myocardium always give trouble for automatic detection. Because of these, we developed a manual correction UI to interactively label the myocardium in an image. The UI enables users to click on image to move local control points which represent the optimal location of local features. The global constraint is automatically enforced to adjust the final ellipse shape according to the changes made by the user. Figure 6 shows that the UI can efficiently and intuitively track the myocardium contour with minimum user interaction.

3 V_e Calculation

After the LV is successfully tracked, we can sample both the myocardium and blood in all images and calculate the T_1 value for them. With T_1 values from both the pre-MOLLI sequence and post-MOLLI sequence, we can compute the V_e index with user-input hematocrit values.

3.1 T_1 Calculation

In order to calculate T_1 value for a tissue, we need to sample the pixel value of the tissue in all images in the MOLLI sequence as

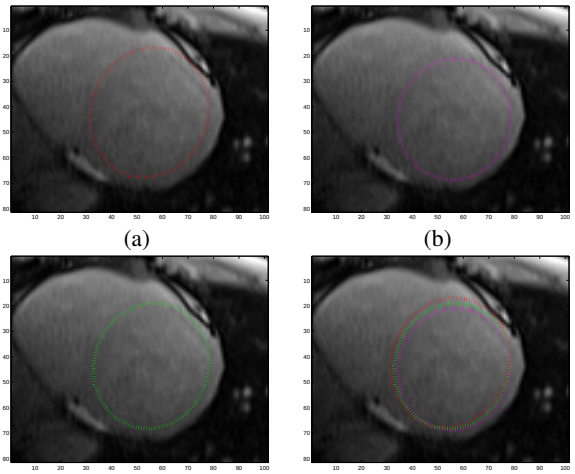

(a) (b) (c) (d)

Figure 5: Cooperative Detection (a) Gradient feature detection result. Upper right portion is attracted by fat on epicardial border. (b) Intensity feature result which is robust on upper right portion however the lower right portion is much closer to the lung. (c) Cooperative result that is more correct in both regions. (d) Overlapped plot of all 3 contour results.

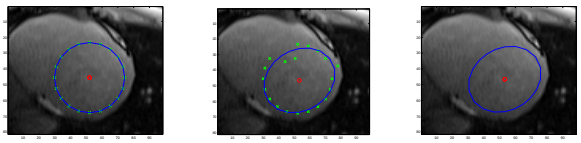

(a) (b) (c)

Figure 6: Interactive correction of detection result (a) an example contour result (b) by setting 3 new control points' positions (green 'x'), global constraint automatically correct the shape (c) final result. Note that control points are not necessarily to be set at myocardium, instead it can serve as a handle to pull or push the global contour to the right location.

well as the TI values when the images are captured. Then we can fit a curve of pixel value vs TI and solve the T_1 value for the tissue.

In each image, we evenly sample n locations along the ellipse for myocardium and at the center of the ellipse for blood. We also provide user interface to select a different region for sampling blood in case there are muscles near the center of LV. At each sample location (x_0, y_0), instead of picking one pixel, we extract a small $w \times h$ window of pixels, or a sub-image. Then the sub-image is modulated with a kernel function before an integration operation to get the final sample value V_p:

$$V_p = \sum_{x,y} I(x,y)K(x-x_0, y-y_0)$$

$$for\ x \in [x_0 - w/2, x_0 + w/2], y \in [y_0 - h/2, y_0 + h/2]$$

The $I(x,y)$ is the pixel value of image I at location (x,y). The $K(x,y)$ is a normalized kernel function. In our case, we use a Gaussian function to emphasize the center pixel but also include surrounding pixels. If using a box function, it equals to average all the pixel values within the small window. At myocardium sample locations we use 3×3 windows while a 9×9 window is used for blood. By using such "kernel sampling" method, we can efficiently reduce sampled pixel value noises.

After sampling, all the sample values V_p's for myocardium sample locations within an image are averaged to a global value. Each image in a MOLLI sequence then generate an average pixel value for myocardium and blood. The average pixel value V of a tissue has the following relation with the inversion time TI when the image is captured:

$$V = |K_1 - K_2 e^{-TI/K_3}|$$

With multiple (V, TI) pairs, we can fit a curve to solve the parameter K_1, K_2 and K_3. Then the T_1 value for the tissue is:

$$T_1 = K_3(\frac{K_2}{K_1} - 1)$$

With the MOLLI sequence, we then can calculate the T_1 for myocardium and blood.

3.2 V_e Calculation and Visualization

To measure the V_e value, we first capture a MOLLI sequence without contrast injection. This sequence is called pre-MOLLI sequence. Then another MOLLI sequence is captured after *Gd* contrast injection. This sequence is called post-MOLLI. Each of the pre and post MOLLI sequence will be processed by our tool and the T_1 values for both myocardium and blood are measured, totally we will have the 4 T_1 values. The V_e then can be computed using equations 1 and 2.

Besides a global V_e value for the whole left ventricle myocardium, our tool can divide the myocardium contour into sections and calculate V_e for each section. This "sectional" V_e values can characterize the local health condition of the LV, bringing more details than a single global V_e, as shown in Figure 7. With this local V_e visualization, doctors can easily see which part of the left ventricle is malfunctioned and quantify how bad it is. This local information could be very useful for diagnosis of some diseases. For example, hypertrophic cardiomyopathy, which is a disease That can cause abnormal thickening of the heart muscle in an asymmetric pattern. So it is important to measure local myocardium tissue property which is not available in a global V_e value.

4 Test and Result

4.1 Test Method

We randomly selected 14 patients' left ventricle short-axis MOLLI scans. Each scan consists of 3 MOLLI sequences: 1 pre sequence and 2 post sequences scanned at different times. Each patient will have 2 V_e values: V_{e_1} and V_{e_2} using the pre sequence and the two the post sequences. The average of these two *Ve* values will be the final result for the patient. We first asked some volunteers from medical school to manually select myocardium pixels and blood pixels to calculate the *Ve*'s. The manual pixel selection result is verified by experienced medical doctors. Then we use our tool to calculate another set of *Ve* values for comparison.

We first measure the consistency of the *Ve* calculation for manual method and our tool's method, which is how similar the V_{e_1} and V_{e_2} values are for the same patient measured by the method. In ideal case, these two values should be the same. However because of image noises there could be some differences. Then we measure the difference for the final *Ve* value generated by the two method for all patients.

4.2 Test Result

The result is shown in table 1. It shows that our tool can achieve much better consistency when measuring *Ve*. Most inconsistency is caused by noise in images and respiratory motion. Because of the sampling method and consistent tracking result, our tool can greatly reduce these effect in calculation of *Ve*. The difference between the two result is similar to the inconsistency measured for manual method. That means statistically they are well correlated.

5 Conclusion and Future Work

In this paper we present a tool to measure the myocardial extracellular volume fraction V_e from CMR images. It uses a global+local myocardium tracking algorithm to automatically identify the location of left ventricle myocardium in short-axis images. By automating the T_1 and V_e calculation, the tool greatly improves the data processing efficiency.

Acknowledgements

Dr. Schelbert is supported by a NIH grant HL102429; a T. Franklin Williams Scholarship Award; Funding provided by: Atlantic Philanthropies, Inc, the John A. Hartford Foundation, the Association of Specialty Professors, and the American Heart Association; and grant from the Pittsburgh Foundation.

References

[1] T. Cootes, C. Taylor, D. Cooper, and J. Graham. Active shape models - their training and application. In *Computer Vision and Image Understanding*, volume 61, pages 38–59, 1995.

[2] T. F. Cootes, G. J. Edwards, and C. J. Taylor. Active apperance models. In *ECCV*, volume 2, pages 484–498, 1998.

[3] R. Devereux, B. Dahlof, E. Gerdts, and et al. Regression of hypertensive left ventricular hypertrophy by losartan compared with atenolol: the losartan intervention for endpoint reduction in hypertension (life) trial. *Circulation*, 110(11):1456–1462, 2004.

[4] A. Flett, M. Hayward, M. Ashworth, M. Hansen, A. Taylor, P. Elliott, C. McGregor, and J. Moon. Equilibrium contrast cardiovascular magnetic resonance for the measurement of diffuse myocardial fibrosis: preliminary validation in humans. *Circulation*, 122(2):138–144, 2010.

[5] R. M. Haralick and L. G. Shapiro. *Computer and Robot Vision, Volume II*. Addison-Wesley, 1992.

[6] M. Jerosch-Herold, D. Sheridan, J. Kushner, D. Nauman, D. Burgess, D. Dutton, R. Alharethi, D. Li, and R. Hershberger. Cardiac magnetic resonance imaging of myocardial contrast uptake and blood flow in patients affected with idiopathic or familial dilated cardiomyopathy. *Am J Physiol Heart Circ Physiol*, 295(3):H1234–H1242, 2008.

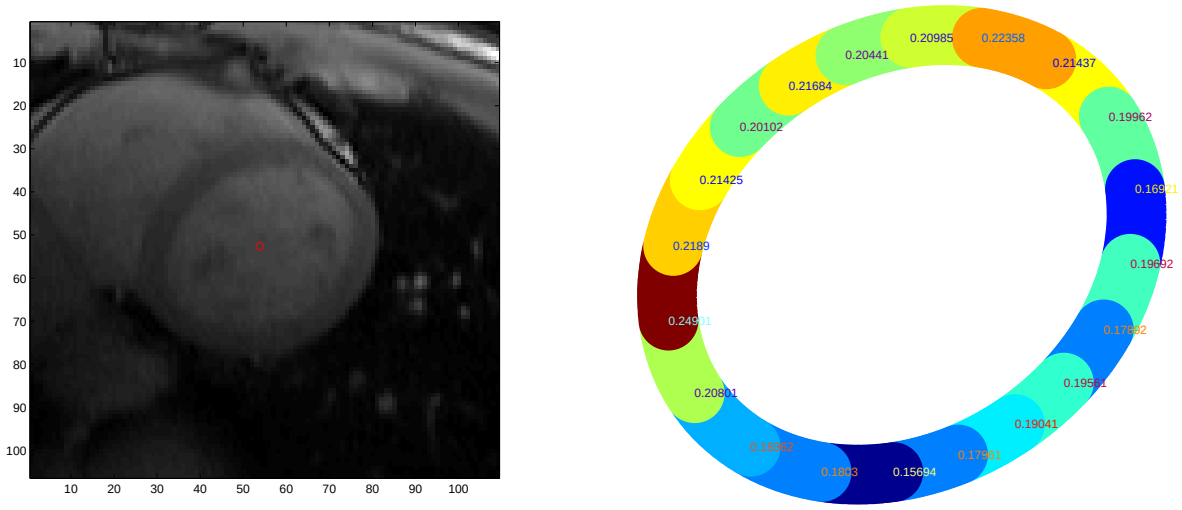

(a) (b)

Figure 7: Multi-bin V_e visualization. (a) the input LV image (b) the visualization of V_e value along the LV myocardium contour. Blue means lower V_e value and red means higher V_e value.

Ve consistency		*Ve* difference
manual result	our tool's result	0.019917 ± 0.013019
0.023055 ± 0.024737	0.010253 ± 0.005972	

(a)

patient	V_{e1}	V_{e2}	mean V_e	mean V_e'	V'_{e1}	V'_{e2}
1	0.33627	0.3506	0.34344	0.32168	0.35282	0.29054
2	0.3306	0.3476	0.3391	0.30347	0.31024	0.29671
3	0.25683	0.24714	0.25199	0.25973	0.26543	0.25404
4	0.21524	0.22577	0.22051	0.22692	0.21663	0.23722
5	0.20461	0.20376	0.20419	0.17885	0.18419	0.17351
6	0.2407	0.25257	0.24663	0.26509	0.30979	0.22039
7	0.29405	0.30696	0.30051	0.26088	0.26918	0.25258
8	0.27872	0.28139	0.28006	0.24651	0.2484	0.24462
9	0.26562	0.28721	0.27642	0.2872	0.26858	0.30582
10	0.31964	0.32992	0.32478	0.31576	0.30463	0.32688
11	0.27221	0.28385	0.27803	0.26317	0.26101	0.26534
12	0.30129	0.30339	0.30234	0.29763	0.29872	0.29655
13	0.27622	0.29004	0.28313	0.2419	0.23177	0.25202
14	0.56175	0.56601	0.56388	0.5736	0.56946	0.57774

(b)

Table 1: (a) Consistency measurement, which is the difference of two *Ve*'s calculated for a same patient and average difference for all patients for the two methods. As shown in the table, the consistency of our method is greater than manual results. And the difference between the result from manual method and our tool is within the consistency measured for manual result. (b) detailed measurement for all 14 patients. V_e is from our tool, V_e' is from manual method.

[7] S. C. Mitchell, J. G. Bosch, B. P. F. Lelieveldt, R. J. van der Geest, J. H. C. Reiber, and M. Sonka. 3-d active appearance models: Segmentation of cardiac mr and ultrasound images. *IEEE Trans. Med. Imaging*, 21(9):1167–1178, 2002.

[8] N. Pack, E. Dibella, B. Wilson, and C. McGann. Quantitative myocardial distribution volume from dynamic contrast-enhanced mri. *Magn Reson Imaging*, 26(4):532–542, 2008.

[9] G. Stanisz and R. Henkelman. Gd-dtpa relaxivity depends on macromolecular content. *Magn Reson Med*, 44(5):665–667, 2000.

[10] K. Weber and C. Brilla. Pathological hypertrophy and cardiac interstitium fibrosis and renin-angiotensin-aldosterone system. *Circulation*, 83(6):1849–1865, 1991.